IRANIAN JOURNAL OF PHYSICS RESEARCH

Iranian Journal of Physics Research, Vol. 12, No. 3, 2012

A Mössbauer effect study, as the main key to the investigation of anomalous magnetic properties of MnZn nanoferrite

M J Nasr Isfahani[1] and V Sepelak[2]

1. Department of Physics, Lenjan Branch, Islamic Azad University, Isfahan, Iran
2. Institute of Nanotechnology, Karlsruhe Institute of Technology, Herrmann-von-Helmholtz-Platz 1, 76344 Eggenstein-Leopoldshafen, Germany
E-mail: m.nasr@iauln.ac.ir

(Received 1 August 2011 , in final from 24 June 2012)

Abstract

In this research, a low temperature in-field ^{57}Fe Mössbauer spectroscopy is used for investigation of anomalous magnetic properties of MnZn nanoferrite. Based on Mössbauer spectroscopy results, the reduced saturation magnetization of MnZn nanoferrite in respect to that of bulk sample is due to nonequilibrium cation distribution and spin disorder. The enhanced Curie temperature of MnZn nanoferrite in respect to that of bulk sample can be attributed to the strengthening of the (A)-O-[B] superexchange interactions due to an increase of the magnetic ion concentration in the (A) site.

Keywords: ferrimagnetic materials, Mössbauer effect, hyperfine interactions

1. Introduction

^{57}Fe Mössbauer spectroscopy is a nuclear-probe technique that is very well suited for the investigation of the local symmetry, the magnetic state, and the charge states of iron ions in iron-containing materials. This sensitivity is due to interactions of the ^{57}Fe nuclei with their surroundings. In spinel ferrites, MFe_2O_4 (M is a divalent metal cation), Mössbauer spectra are often dominated by magnetic interactions. The splitting of the characteristic six line spectra reveals the local magnetic fields at the positions of the Mössbauer nuclei. At room and at lower temperatures, these fields often are of the order of 50 T [1]. The origin of such high local fields in spinel ferrites is due to an indirect-exchange interaction (superexchange) between nuclear spins, where the spin density is transferred via the oxygen anions [2]. As a consequence of this supertransfer mechanism, a particular iron ion experiences local fields that reflect the distribution of magnetic (ferric) ions in its neighborhood. This is particularly true for ions in octahedral coordination [2].

The ability to readily provide information about the noncollinearity of spins in magnetic structures is one of the great advantages of Mössbauer spectroscopy. The relative intensities of second (I_2) and fifth (I_5) lines in magnetically split six-line spectra depend on the angle between the magnetic hyperfine field and the gamma ray direction [2]. Thus, by applying an external magnetic field with sufficient strength, one can study the degree of alignment of the spins along the field direction. When the aligned moments are composed of canted local spin moments, the directions of the magnetic hyperfine fields are no longer parallel to the external field and both I_2 and I_5 will change. The canting angle θ can be calculated from the line intensities of the magnetically split Mössbauer spectra.

The magnetic moments of the nanoscale mechanically treated ferrite particles undergo, above a certain temperature, spontaneous thermal fluctuations, analogous to the behavior of paramagnetic atoms, and exhibit a so-called superparamagnetic behavior [3]. Because of its great sensitivity to these magnetic fluctuations, Mössbauer spectroscopy was found to be a suitable technique for their detection. Such magnetic fluctuations can, however, complicate the analysis of spectra by a collapse of the magnetic hyperfine field far below the Néel temperature and give rise to relaxation line broadening or—even down to very low temperatures—to unresolved hyperfine-field distributions.

Quadrupolar interactions of the Mössbauer nuclei reflect local symmetry. Here, the symmetry of the charge distribution experienced through the electric field gradients sets up the charges surrounding the nuclei. In the case of ferric ions, this interaction is dominated by

the distribution of ionic charges in the lattice. On the other hand, the isomer shift interaction reflects the electron density at the nuclei. This interaction causes a marked dependence of the position of the Mössbauer transition on the charge state of the Mössbauer ion [4] and, to a lesser extent, on the geometry of its coordination.

The spinel structure consists of an almost perfect fcc arrangement of anions, wherein cations are located in sites of tetrahedral and octahedral coordination forming an ordered array in the interstices provided by the anions. Thus, the structural formula of a spinel ferrites in detail reads $(M^{2+}_{1-\lambda}Fe^{3+}_{\lambda})$ $[M^{2+}_{\lambda}Fe^{3+}_{2-\lambda}]$ O_4, where the round and square brackets enclose species in sites of tetrahedral (A) and octahedral [B] coordination, respectively; λ represents the so-called degree of inversion [defined as the fraction of the (A) sites occupied by Fe^{3+} cations]. In the structure, each tetrahedrally coordinated cation is surrounded by twelve [B]-site ions (each oxygen ion is surrounded by three [B]-site ions). On the other hand, each cation at a [B] site has six (A)-site nearest neighbors [5].

A characteristic property of the supertransfer mechanism in spinel ferrites is given by its strong dependence on the extent to which the spin density is transferred from one interacting cation to another via an intermediate ion. This causes a dependence of local magnetic fields on the cation–anion distance and on the angle formed by the two interacting cations and the intervening oxygen ion. The supertransfer mechanism is most effective if the two cations involved are located on opposite sides of an anion, forming an angle of 180º. Although this configuration does not occur in spinel ferrites, it has been found that the (A)-O-[B] angle of about 126º still results in a significant interaction. On the other hand, the 90º [B]-O-[B] and, in particular, the (A)-O-(A) interaction is magnetically less favorable either because of the smaller angles involved or because of the larger cation–anion distances [6]. The more covalent character of the Fe^{3+}(A)-O bond compared to the Fe^{3+}[B]-O bond explains qualitatively why the spin density transfer from (A) to [B] in the spinel structure is much more effective than vice versa [7]. As a consequence, the octahedrally coordinated ferric ions, Fe^{3+}[B], are very sensitive to the number of their (A)-site nearest magnetic neighbors, Fe^{3+}(A). In contrast, local magnetic fields experienced by Fe^{3+}(A) are virtually independent of the detailed distribution of magnetic ions in the structure.

Among different magnetic materials, Zn-substituted spinel ferrites are attractive because Zn substitution can alter their magnetic parameters in a relatively wide range [8]. For example, MnZn ferrites are technologically important materials because of their high magnetic permeability and low core losses. These ferrites have been widely used in electronic applications such as transformers, choke coils, noise filters, recording heads, etc. [9].

In previous papers, we reported preparation procedure of nanocrystalline $Mn_{0.5}Zn_{0.5}Fe_2O_4$ via high-energy ball milling of the mixture of two single-phase ferrites, $MnFe_2O_4$ and $ZnFe_2O_4$ and Mössbauer studies [10], magnetic properties and morphology of nanocrystalline $Mn_{0.5}Zn_{0.5}Fe_2O_4$ [11]. It is interesting to mention that the magnetization of the mechanosynthesized $Mn_{0.5}Zn_{0.5}Fe_2O_4$ estimated the value of the saturation magnetization of mechanosynthesized $Mn_{0.5}Zn_{0.5}Fe_2O_4$ to be approximately 82.7 emu/g, which is about 41% lower than the value reported for bulk $Mn_{0.5}Zn_{0.5}Fe_2O_4$ (140 emu/g) [11].

The second important observation is that the mechanosynthesized $Mn_{0.5}Zn_{0.5}Fe_2O_4$ exhibits an enhanced Néel temperature. The Néel temperature of $Mn_{0.5}Zn_{0.5}Fe_2O_4$ nanoparticles is estimated to be about 583 K. This value is considerably higher than that reported for bulk $Mn_{0.5}Zn_{0.5}Fe_2O_4$ (413 K) [11].

The present work represents a continuation of our previous works [10, 11] with the following goal:
Investigation of the origin of both the reduced saturation magnetization and the enhanced Néel temperature of mechanosynthesized $Mn_{0.5}Zn_{0.5}Fe_2O_4$, compared with the bulk $Mn_{0.5}Zn_{0.5}Fe_2O_4$.

To elucidate this anomalous behaviour, we performed low-temperature in-field ^{57}Fe Mössbauer measurements. These experiments enable us to determine both ionic configuration and spin arrangement in the mechanosynthesized MnZn ferrite nanoparticles.

2. Experimental procedure

The mechanochemical processing was used for the preparation of nanosized $Mn_{0.5}Zn_{0.5}Fe_2O_4$. $MnFe_2O_4$ and $ZnFe_2O_4$ were used as starting materials. Details of the mechanosynthesis of $Mn_{0.5}Zn_{0.5}Fe_2O_4$ are given in Ref. [10].

^{57}Fe Mössbauer spectroscopic measurements were performed in transmission geometry using a ^{57}Co/Rh γ-ray source. High-field Mössbauer measurements were carried out at 4.2 K in an external magnetic field of 7 T applied parallel to the γ-ray direction. The velocity scale was calibrated relative to ^{57}Fe in Rh. 'Recoil' spectral analysis software [12] was used for the quantitative evaluation of the Mössbauer spectra. The degree of inversion was calculated from the subspectral intensities ($I_{(A)}/I_{[B]}=\lambda/(2-\lambda)$). The average canting angle, ψ, was calculated from the ratio of the intensities of lines 2 and 1, $I_{2,1}$, according to $\psi=90^o-\arcsin[(3I_{2,1}/2)/(1+3I_{2,1}/4)]^{1/2}$ [13].

3. Results and discussions

The low-temperature (4.2 K) Mössbauer spectra of mechanosynthesized $Mn_{0.5}Zn_{0.5}Fe_2O_4$, taken in zero applied magnetic fields and in a magnetic field of 7 T applied parallel to the γ-ray direction are compared in Figure 1. As is clearly seen, the thermal fluctuations are suppressed at 4.2 K, and the Mössbauer spectrum of nanocrystalline $Mn_{0.5}Zn_{0.5}Fe_2O_4$ consists of sextets only. Although the influence of superparamagnetic relaxation is counteracted, a determination of the cation distribution in $Mn_{0.5}Zn_{0.5}Fe_2O_4$ nanoparticles is impossible to make from the low-temperature spectrum at H_{ext} = 0 T (figure

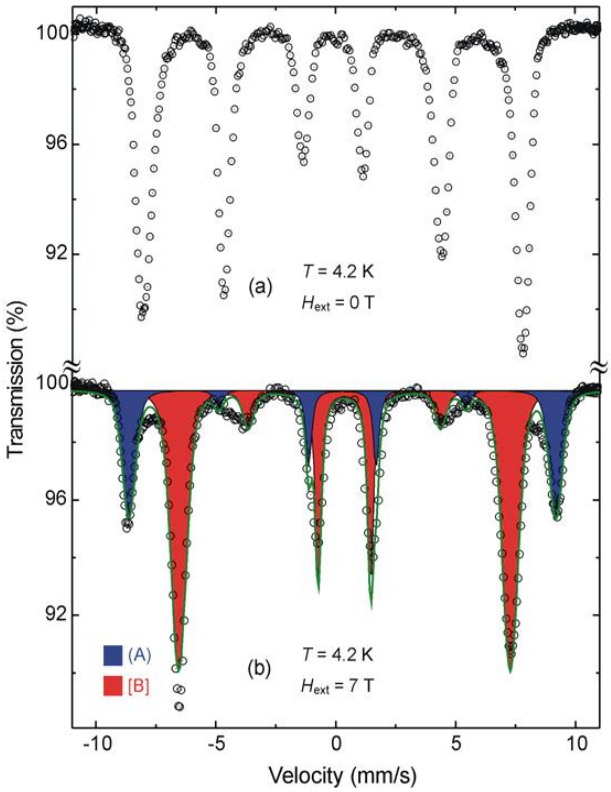

Figure 1. Low-temperature (4.2 K) Mössbauer spectra of nanosized mechanosynthesized $Mn_{0.5}Zn_{0.5}Fe_2O_4$ taken (a) in zero applied magnetic field and (b) in external magnetic field of 7 T applied parallel to the γ-ray direction. Blue and red subspectra correspond to Fe^{3+} cations in tetrahedral (A) and octahedral [B] coordination of oxygen ions, respectively.

1 (a)) because it is difficult to resolve the subspectra to assign them to the respective lattice sites. In the presence of an external magnetic field of H_{ext} = 7 T, the effective magnetization of the individual particles is aligned along the field. As a consequence of the antiparallel alignment of the spins of Fe^{3+} cations at (A) and [B] sites in spinel ferrites, the external field adds to the magnetic hyperfine field at (A) sites and subtracts from the hyperfine field at [B] sites [6]. Because of this fact, the high-field Mössbauer spectrum of nanosized mechanosynthesized $Mn_{0.5}Zn_{0.5}Fe_2O_4$ exhibits the completely resolved (A) and [B] subspectra (see figure 1 (b)). Thus, the use of the large external magnetic fields creates an effective separation of the subpatterns, thereby allowing for an accurate determination of the cation distribution. The hyperfine parameters of (A) and [B]-site ferric ions resulting from the least-squares fitting of the spectrum of nanosized $Mn_{0.5}Zn_{0.5}Fe_2O_4$ are presented in Table 1. The degree of inversion of the mechanosynthesized $Mn_{0.5}Zn_{0.5}Fe_2O_4$ was found to be λ = 0.555(4).

If the external magnetic field H_{ext} is applied parallel to the γ-ray direction, the second and fifth lines of the six-line Mössbauer spectrum vanish for fully collinear magnetic structures [2]. However, figure 1 (b) indicates that in the present study the intensity ratio of the second (or fifth) line to the first (or sixth) line, $I_{2,5}/I_{1,6}$, takes small values for both (A) and [B] subspectra. This

Table 1. Hyperfine parameters (IS – isomer shift, H_{eff} – effective magnetic field, I – relative intensity, $I_{2,5}/I_{1,6}$ – intensity ratio of the second (or fifth) line to the first (or sixth) line, Ψ – average spin canting angle, H – magnetic hyperfine field) obtained by fitting the low-temperature in-field Mössbauer spectrum of nanocrystalline mechanosynthesized $Mn_{0.5}Zn_{0.5}Fe_2O_4$.

Parameter	Fe^{3+} (A)	Fe^{3+} [B]
IS (mm/s)	0.262(1)	0.369(5)
I (%)	27.77(7)	72.23(7)
$I2,5/I1,6$	0.106(9)	0.120(8)
Ψ (°)	22.6(5)	24.0(7)
Heff (T)	55.30(4)	42.90(1)
H (T)	48.91(2)	49.37(7)

implies that Fe-spins in the (A) and [B] sites of the mechanosynthesized material are strongly canted under the applied field. The obtained intensity ratios $I_{2,5}/I_{1,6}$ for each subspectrum are also listed in Table 1. The average canting angles, characterizing noncollinear spin arrangement of Fe^{3+} ions on (A) and [B] sites in the mechanosynthesized ferrite, were found to be Ψ(A) = 22.6(5)° and Ψ[B] = 24.0(7)°, respectively. Thus, the spins located on the two sublattices in the mechanosynthesized material are found to behave slightly different in the external field of 7 T. This result is also consistent with previous works, where different spin canting in the (A) and [B] sublattices of spinel nanostructures was observed [14-17].

The effective magnetic fields H_{eff}(A) and H_{eff}[B] observed at the ^{57}Fe nuclei in (A) and (B) sites of mechanosynthesized $Mn_{0.5}Zn_{0.5}Fe_2O_4$, respectively, are listed in Table 1. Note that the effective magnetic field is the vector sum of the magnetic hyperfine field (H) and the applied field H_{ext} [18]. The values of the magnetic hyperfine field (listed in Table 1) were estimated from those of the effective magnetic field and external magnetic field using the relationship $H^2 = H_{eff}^2 + H_{ext}^2 \pm 2H_{eff}H_{ext}\cos\Psi$ [15], where – and + are for (A) and [B] spectral components, respectively. It is found that the magnetic hyperfine fields experienced by Fe^{3+} ions located in the (A) and [B] sites of the mechanosynthesized material are very similar (H(A) = 48.91(2) T and H[B] = 49.37(7) T); thus, it would be impossible to resolve the (A) and [B] subspectra even at low temperatures without application of an external magnetic field (see also figure 1 (a)).

Based on the quantitative results of the low-temperature in-field ^{57}Fe Mössbauer measurements, it can be stated that the atomic and spin configurations in the mechanosynthesized $Mn_{0.5}Zn_{0.5}Fe_2O_4$ are characterized by a nonequilibrium cation distribution and noncollinear spin alignment, respectively. Taking into account that Zn^{2+} ions have a strong preference for (A) sites in spinels [19], the crystal chemical formula of the mechanosynthesized ferrite can therefore be written as $(Zn_{0.44}Fe_{0.56}\searrow)[Zn_{0.06}Mn_{0.50}Fe_{1.44}\nearrow]O_4$. Compared with the core–shell configuration of mechanosynthesized

complex oxides [20-22], it can be assumed that both nonequilibrium cation distribution and canted spins are located in the surface shell regions of the $Mn_{0.5}Zn_{0.5}Fe_2O_4$ nanoparticles. Note that the cation distribution in the bulk Mn-Zn ferrite can be described by the following crystal chemical formula: $(Zn_{0.50}Mn_{0.5})[Fe_2\uparrow]O_4$ [23].

The quantitative information on the ion configuration and the spin structure, obtained from the analysis of Mössbauer spectra, is very helpful in the interpretation of both the reduced saturation magnetization Ms and the enhanced Néel temperature T_N of mechanosynthesized $Mn_{0.5}Zn_{0.5}Fe_2O_4$. Since Zn^{2+} ions possess no magnetic moment, the total magnetic moment μ in $Mn_{0.5}Zn_{0.5}Fe_2O_4 \equiv (Zn_xMn_yFe_\lambda)[Zn_{0.5-x}Mn_{0.5-y}Fe_{2-\lambda}]O_4$ is entirely due to the uncompensated magnetic moments of Fe^{3+} and Mn^{2+} ions. Thus, from the λ and Ψ values, the effective magnetic moment (per formula unit) of $Mn_{0.5}Zn_{0.5}Fe_2O_4$ can be calculated as:

$\mu = \mu_{[B]} - \mu_{(A)} = [(2 - \lambda)\ \mu_{Fe} \cos\Psi_{[B]} + (0.5 - y)\ \mu_{Mn} \cos\Psi_{[B]Mn}] - (\lambda\ \mu_{Fe} \cos\Psi_{(A)} + y\ \mu_{Mn} \cos\Psi_{(A)Mn})$

Where μ_{Fe} and μ_{Mn} are magnetic moments of Fe^{3+} and Mn^{2+} ions, respectively: $\mu_{Fe} = \mu_{Mn} = 5\ \mu_B$. The values λ = 0, x = 0.5, y = 0.5, and $\Psi_{(A)} = \Psi_{[B]} = 0°$, characteristic of the bulk Mn-Zn ferrite [23], result in the magnetic moment $\mu_{bulk} = 7.50\ \mu_B$/f.u.. On the other hand, the values λ = 0.56, x = 0.44, y = 0, and $\Psi_{(A)} = 22.6°$, $\Psi_{[B]} = \Psi_{[B]Mn} = 24.0°$ (the same canting angles are assumed for Fe^{3+} and Mn^{2+} spins in [B] sites), characteristic of the mechanosynthesized material, lead to the effective magnetic moment $\mu_{nano} = 6.28\ \mu_B$/f.u.. Thus, the disordered cation and spin configurations theoretically lead to the M_s value that is approximately 1.2 times smaller than that of the ordered bulk material. This is in reasonable agreement with the results of magnetization measurements, which demonstrate that Ms of mechanosynthesized $Mn_{0.5}Zn_{0.5}Fe_2O_4$ is about 1.7 times smaller than that calculated for the bulk material. Thus, the theoretical considerations presented above clearly demonstrate that the origin of the reduced Ms of mechanosynthesized Mn-Zn ferrite lies in both nonequilibrium cation distribution and spin disorder. Compaerd with other mechanosynthesized spinel ferrites, the magnetic degradation observed in the present case can be attributed to the nonequilibrium cation and noncollinear spin effects in the surface shell of $Mn_{0.5}Zn_{0.5}Fe_2O_4$ nanoparticles [20, 21].

Taking into account the crystal chemical formulas of $(Zn_{0.50}Mn_{0.5})[Fe_2]O_4$ and $(Zn_{0.44}Fe_{0.56})[Zn_{0.06}Mn_{0.50}Fe_{1.44}]O_4$, characteristic of bulk and nanocrystalline Mn-Zn ferrites, respectively, it is evident that the mechanosynthesized ferrite possesses a larger number of the (A)-O-[B] exchange paths. This is directly related to the Néel temperature of the ferrite system [14]. The enhanced T_N observed for the mechanosynthesized material can therefore be attributed to the strengthening of the (A)-O-[B] superexchange interaction due to an increase of the magnetic ion concentration in the (A) site [24-25].

4. Conclusions

A low temperature in-field ^{57}Fe Mössbauer spectroscopy has proved a powerful technique for the elucidation of atomic local structure in MnZn nanoferrite and of the changes in their cation distributions brought about by mechanical activation. Based on Mössbauer spectroscopy results, the reduced saturation magnetization in respect to the bulk sample is due to nonequilibrium cation distribution and spin disorder. The enhanced Curie temperature of MnZn nanoferrite compaerd with bulk sample can be attributed to the strengthening of the (A)-O-[B] superexchange interactions due to an increase of the magnetic ion concentration in the (A) site.

Acknowledgments

M.J.N.I is grateful to the Iranian Nanotechnology Initiative. V.Š. gratefully acknowledges the support by the DFG and VEGA.

References

1. G A Sawatzky, F Van Der Woude, and A H Morrish, *Phys. Rev*. **187** (1969) 747.
2. R E Vandenberghe, and E De Grave, "*In Mössbauer Spectroscopy Applied to Inorganic Chemistry*," G. J. Long and F. Grandjean, eds. Plenum Press, New York, **3** (1989) 59.
3. S Mørup, "*In Mössbauer Spectroscopy Applied to Inorganic Chemistry*," G. J. Long, ed. Plenum Press, New York, **2** (1987) 89.
4. F Menil, *J. Phys. Chem. Solids* **46** (1985) 763.
5. R Valenzuela, "*Magnetic Ceramics*" Cambridge University Press, Cambridge (1994).
6. F Grandjean, "*In Mössbauer Spectroscopy Applied to Inorganic Chemistry*," G. J. Long, ed. (Plenum Press, New York, **2** (1987) 241.
7. F Van Der Woude, and G A Sawatzky, *Phys. Rev*. B **4** (1971) 3159.
8. H W Wang, and S C Kung, *J. Magn. Magn. Mater*. **270** (2004) 230.
9. C C Hwange, J S Tasi, T H Huang, C H Peng, and S Y Chen, *J. Solid State Chem*. **178** (2005) 382.
10. M J Nasr Isfahani, M Myndyk, V Šepelák, and J. Amighian, *J. Alloy. Compd*. **470** (2009) 434.
11. M J Nasr Isfahani, M Myndyk, D Menzel, A Feldhoff, J Amighian, V Šepelák, and *J. Magn. Magn. Mater*. **321** (2009) 152.
12. K Lagarec, and D G Rancourt, "*Recoil - Mössbauer Spectral Analysis Software for Windows*," version 1.02; Department of Physics, University of Ottawa, Ottawa (1998).
13. A Pantelouris, H Modrow, M Pantelouris, J Hormes, and D Reinen, *Chem. Phys*. **300** (2004) 13.
14. N Ponpandian, A Narayanasamy, C N Chinnasamy, N Sivakumar, J-M Greneche, K Chattopadhyay, K

Shinoda, B Jeyadevan, and K Tohji, *Appl. Phys. Lett*. **86** (2005) 192510.
15. Ö Helgason, J-M Greneche, F J Berry, and F Mosselmans, *J. Phys. Condens. Matter*. **15** (2003) 2907.
16. R N Bhowmik, R Ranganathan, S Sarkar, C Bansal, and R Nagarajan, *Phys. Rev*. B **68** (2003) 134433.
17. G F Goya, and E R Leite, *J. Phys. Condens. Matter*. **15** (2003) 641.
18. E J Choi, Y Ahn, and K-C Song, *J. Magn. Magn*. Mater. **301** (2006) 171.
19. P Druska, U Steinike, and V Šepelák, *J. Solid State Chem*. **146** (1999) 13.
20. V Šepelák, I Bergmann, A Feldhoff, P Heitjans, F Krumeich, D Menzel, F J Litterst, S J Campbell, and K D Becker, *J. Phys. Chem*. C **111** (2007) 5026.
21. V Šepelák, A Feldhoff, P Heitjans, F Krumeich, D Menzel, F J Litterst, I Bergmann, and K D Becker, *Chem. Mater*. **18** (2006) 3057.
22. V Šepelák, K D Becker, I Bergmann, S Suzuki, S Indris, A Feldhoff, P Heitjans, and C P Grey, *Chem. Mater*. **21** (2009) 2518.
23. A H Morrish, and P E Clark, *Phys. Rev*. B **11** (1975) 278.
24. A Yang, C N Chinnasamy, J M Greneche, Y Chen, S D Yoon, K Hsu, C Vittoria, and V G Harris, *Appl. Phys. Lett*. **94** (2009) 113109.
25. N Sivakumar, A Narayanasamy, N Ponpandian, J-M Greneche, K Shinoda, B Jeyadevan, and K Tohji, *J. Phys*. D: *Appl. Phys*. **39** (2006) 4688.